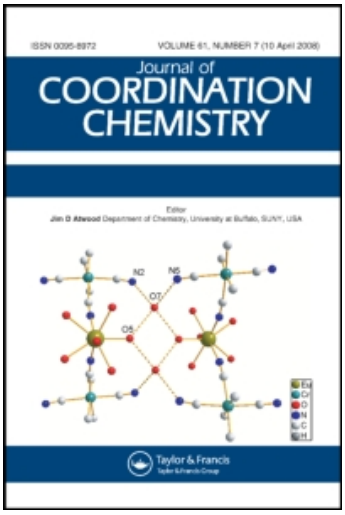

Journal of Coordination Chemistry
Publication details, including instructions for authors and subscription information:
http://www.informaworld.com/smpp/title~content=t713455674

Ni(II) benzylbutyldithiocarbamates containing monodentate phosphines

Richard Pastorek[a]; Jiří Kameníček[a]; Josef Husárek[a]; Václav Slovák[b]; Marek Pavlíček[a]
[a] Department of Inorganic Chemistry, Palacký University, 77147 Olomouc, Czech Republic [b] Faculty of Science, Department of Chemistry, University of Ostrava, 70103 Ostrava, Czech Republic

To cite this Article Pastorek, Richard , Kameníček, Jiří , Husárek, Josef , Slovák, Václav and Pavlíček, Marek(2007) 'Ni(II) benzylbutyldithiocarbamates containing monodentate phosphines', Journal of Coordination Chemistry, 60: 5, 485 — 494
To link to this Article: DOI: 10.1080/00958970600794966
URL: http://dx.doi.org/10.1080/00958970600794966

Journal of Coordination Chemistry
Vol. 60, No. 5, 10 March 2007, 485–494

Taylor & Francis
Taylor & Francis Group

Ni(II) benzylbutyldithiocarbamates containing monodentate phosphines

RICHARD PASTOREK†, JIŘÍ KAMENÍČEK*†, JOSEF HUSÁREK†, VÁCLAV SLOVÁK‡ and MAREK PAVLÍČEK†

†Department of Inorganic Chemistry, Palacký University, Křížkovského 10, 77147 Olomouc, Czech Republic
‡Faculty of Science, Department of Chemistry, University of Ostrava, 30. dubna 22, 70103 Ostrava, Czech Republic

(*Received in final form 5 March 2006*)

Ni(II) benzylbutyldithiocarbamate complexes containing monodentate phosphines of composition $[Ni(BzBudtc)_2]$, $[NiX(BzBudtc)(PPh_3)]$, $[Ni(BzBudtc)(PPh_3)_2]Y$ and $[Ni(BzBudtc)(PBu_3)_2]Y$ {X = Cl, Br, I, NCS; Y = ClO_4, PF_6, BPh_4; BzBudtc = benzylbutyldithiocarbamate, PPh_3 = triphenylphosphine, PBu_3 = tributylphosphine} have been synthesized. They were characterized by elemental and thermal analysis, IR, electronic and $^{31}P\{^1H\}$ NMR spectroscopy, magnetochemical and conductivity measurements. Single crystal X-ray analyses of $[NiCl(BzBudtc)(PPh_3)]$ and $[Ni(BzBudtc)(PPh_3)_2]PF_6 \cdot 0.5CH_3OH$ confirmed coordination number four for nickel with distorted square coordination spheres for NiS_2PCl and NiS_2P_2 chromophores. For selected samples, their catalytic influence on graphite oxidation was studied.

Keywords: Nickel(II); Dithiocarbamate; X-ray structure; Graphite oxidation

1. Introduction

In the past literature, there are only two references describing unsymmetrical Ni(II) dithiocarbamates of the $[Ni(R_1R_2dtc)_2]$ type containing monodentate phosphines, $[Ni(MeEadtc)(PPh_3)_2]ClO_4$ (MeEadtc = methyl-2-hydroxyethyldithiocarbamate) [1] and $[Ni(MeGlydtc)(PPh_3)_2]ClO_4$ (MeGlydtc = methylcarboxymethyldithiocarbamate) [2]. Recently, we reported the complexes $[NiX(Bz^iPrdtc)(PPh_3)]$, (X = Cl, Br, I, NCS; Bz^iPrdtc = benzylisopropyldithiocarbamate) [3], $[Ni(Bz^iPrdtc)(PPh_3)_2]Y$ (Y = ClO_4, PF_6, BPh_4) [4], $[Ni(CyEtdtc)(PPh_3)_2]Y$ (Y = ClO_4, PF_6, BPh_4; CyEtdtc = cyclohexylethyldithiocarbamate) [4]; $[Ni(CyEtdtc)(PBu_3)_2]Y$ (Y = ClO_4, BPh_4) [4], $[NiX(BzBudtc)(PBu_3)]$ (X = Cl, Br, NCS; BzBudtc = benzylbutyldithiocarbamate) [5] and $[NiX(CyEtdtc)(PR_3)]$ (X = Cl, Br, I, NCS; R = Ph, Bu) [6]. Single crystal X-ray analysis of $[Ni(MeEadtc)(PPh_3)_2]ClO_4$ [1], $[NiX(Bz^iPrdtc)(PPh_3)]$ (X = Br, I) [3], $[NiCl(Bz^iPrdtc)(PPh_3)] \cdot CHCl_3$ [3] and $[Ni(Bz^iPrdtc)(PPh_3)_2]ClO_4 \cdot 0.5H_2O$ [4] confirmed that NiS_2PX

*Corresponding author. Email: kamen@prfnw.upol.cz

ISSN 0095-8972 print/ISSN 1029-0389 online © 2007 Taylor & Francis
DOI: 10.1080/00958970600794966

and NiS_2P_2 chromophores are approximately square planar. As for Ni(II) benzylbutyldithiocarbamates, no literature data are available.

Here, the syntheses of of $[NiX(BzBudtc)(PPh_3)]$ and $[Ni(BzBudtc)(PR_3)_2]Y$ complexes (BzBudtc = benzylbutyldithiocarbamate; R = Ph, Bu) are described. For selected samples, we used thermal analysis to study their catalytic influence on graphite oxidation. Application possibilities of these results have been discussed elsewhere [7, 8].

2. Experimental

All chemicals used were commercially available, of analytical quality and used as supplied.

2.1. *Syntheses*

2.1.1. [Ni(BzBudtc)$_2$] (I). The complex was obtained by reaction of CS_2 (100 mmol) with benzylbutylamine (100 mmol) in ethanol (96%, 50 cm^3). After addition of a warm solution of $NiCl_2 \cdot 6H_2O$ (50 mmol in 100 cm^3 water) during 1 h, the dark green precipitate of $[Ni(BzBudtc)_2]$ was separated by filtration, washed with warm water to remove Cl^-, and dried at 40°C under an infrared lamp (Yield: 43%).

2.1.2. [NiX(BzBudtc)(PPh$_3$)] {X = Cl(II), Br(III), I(IV), NCS(V)}. A suspension of finely powdered $[Ni(BzBudtc)_2]$ (1 mmol) and $[NiX_2(PPh_3)_2]$ (1 mmol) [9] in chloroform (10 cm^3) was stirred at room temperature until all components dissolved. The red-violet solutions were filtered and addition of excess amount of diethylether lead to the formation of solid phases during 2 days. They were separated by filtration, washed with diethylether, and dried under an infrared lamp at 40°C. Yields: 68% (**II**); 62% (**III**); 55% (**IV**); 69% (**V**). Crystals of complex **II** suitable for X-ray analysis were obtained by recrystallization from diethylether.

2.1.3. [Ni(BzBudtc)(PR$_3$)$_2$]Y {Y = ClO$_4$(VI, IX); PF$_6$(VII, X); BPh$_4$(VIII, XI); R = Ph, Bu}. A suspension of finely powdered $[Ni(BzBudtc)_2]$ (1 mmol), PR_3 (2 mmol) and $NiCl_2 \cdot 6H_2O$ (0.5 mmol) in 30 cm^3 of methanol was stirred under reflux for 2 h. Finely powdered $NaClO_4 \cdot H_2O$ (alternatively KPF_6 or $NaBPh_4$; 1 mmol) was then added and the mixture stirred under reflux for 1 h. For **VIII**, an orange solid was recrystallized from methanol and washed with water and petroleum ether. For **VI** and **VII**, filtration through active carbon was necessary and during two days, red crystals formed (for **VII**, a crystal suitable for X-ray analysis was selected). The final products were washed with water and petroleum ether. For **IX**, **X**, **XI**, evaporation to near dryness gave solids that were redissolved in water and precipitated by addition of petroleum ether. All samples were dried under an infrared lamp at 40°C. Yields: 35% (**VI**); 32% (**VII**); 36% (**VIII**); 35% (**IX**); 28% (**X**); 31% (**XI**).

2.2. *Physical measurements*

Nickel contents were determined by chelatometric titration using murexide as indicator [10]. Chlorine, bromine and iodine were determined by the

Schöniger method [11]. CHNS analyses were performed on an Fisons EA 1108 instrument. Satisfactory analyses for all complexes were obtained. Room temperature magnetic susceptibilities were measured by the Faraday method using $Co[Hg(NCS)_4]$ as calibrant on a laboratory-designed instrument using a Sartorius 4434 MP-8 balance. Conductivities were measured with an LF 330 meter (WTW GmbH) at 25°C. Diffuse reflectance electronic spectra (40,000–11,000 cm^{-1}) were recorded on a Specord M 40 spectrophotometer and IR spectra (4000–400 cm^{-1}) on a Specord M 80 instrument using nujol mulls. $^{31}P\{^1H\}$ NMR spectra were measured on a Bruker Avance 300 spectrometer, operating at frequency of 121.44 MHz. All samples were prepared by dissolving the compounds in $CDCl_3$ and measurements were performed at 300 K; 85% H_3PO_4 was used as external standard. Thermal analysis was performed on a Seiko 6200 TG/DTA instrument; heating rate 2.5°C min^{-1}, sample weight 9–11 mg, temperature range 20–1000°C.

Catalytic graphite oxidation studies were carried out on a Netzsch STA 449C device with a standardless α-Al_2O_3 crucible and with a heating rate of 10°C min^{-1}, a sample weight of 5.0–5.2 mg and in dynamic atmosphere (air, 100 cm^3 min^{-1}). Samples were obtained by mixing graphite (0.6 g, diameter of particles less than 0.1 mm, ash residue max. 0.2%, mass drying loss max. 0.2%) and an acetone solution (2 cm^3) of the appropriate complexes **I**, **IV**, **VI**, and **X**; $[Ni] = 2.5 \times 10^{-3}$ mol dm^{-3} and pure acetone (sample **0**; see below). All samples were homogenized by stirring and dried at room temperature for 24 h. Kinetic parameters were calculated by a direct non-linear regression method [12].

2.3. *Crystal structure*

X-ray data collection for **II** and **VII** was performed on an Oxford Diffraction Xcalibur^{TM}2 four circle κ-axis diffractometer equipped with a Sapphire2 CCD detector, monochromator Enhance and a Cryojet cooler system, using Mo-Kα radiation at 100 K. The CrysAlis program package (V 1.171.7, Oxford Diffraction) was used for data reduction. Both structures were solved by heavy atom methods using SHELXS-97 [13] and refined anisotropically for all non-hydrogen atoms by full-matrix least-squares procedures using SHELXL-97 [14]. For **VII**, a DIFABS absorption correction [15] was applied. All hydrogen atoms and disordered C and O atoms of **VII** were refined isotropically. Additional calculations were performed using the PARST program [16]. X-ray data are summarized in tables 1–3.

3. Results and discussion

Important physical data for all complexes are summarized in table 4. All complexes are diamagnetic. Compounds $[Ni(BzBudtc)_2]$ and $[NiX(BzBudtc)(PPh_3)]$ are non-electrolytes and complexes $[Ni(BzBudtc)(PR_3)_2]Y$ are 1 : 1 electrolytes. This is in accord with the assumption of a square planar arrangement of the coordination sphere (NiS_4, NiS_2PX and NiS_2P_2 chromophores). The ionic nature of the Y^- anion in $[Ni(BzBudtc)(PR_3)_2]Y$ was supported by IR spectra. For **VI** and **IX** with $Y = ClO_4^-$ non-split peaks (ν_3) appeared at 1089 and 1065 cm^{-1}, ν_4 at 615 and 620 cm^{-1} [17]; for $Y = PF_6^-$ (**VII**, **X**) bands at 835 and 830 cm^{-1} were found [18]. For **V**, the coordination of NCS to the central nickel atom *via* nitrogen atom {ν(C≡N) at 2090 cm^{-1} and ν(C–S)

Table 1. Crystal data and structure refinement details for [NiCl(BzBudtc)(PPh_3)] and [Ni(BzBudtc)(PPh_3)$_2$]$PF_6 \cdot 0.5CH_3OH$.

Empirical formula	$C_{30}H_{31}ClNNiPS_2$	$C_{48.5}H_{46}F_6NNiO_{0.5}P_3S_2$
Formula weight	594.81	980.60
Temperature (K)	100(2)	100(2)
Wavelength (Å)	0.71069	0.71069
Crystal system, space group	$P\bar{1}$	$P\bar{1}$
Unit cell dimensions (Å, °)		
a	11.006(5)	13.063(3)
b	11.396(5)	13.176(3)
c	12.533(5)	14.981(3)
α	73.830(5)	95.83(3)
β	88.390(5)	111.49(3)
γ	71.370(5)	92.63(3)
Volume (Å^3)	1427.4(11)	2377.2(9)
Z; Calculated density (Mg m^{-3})	2; 1.384	2; 1.370
F(000); Absorption coefficient (mm^{-1})	620; 0.996	1014; 0.656
Crystal size (mm^3)	$0.4 \times 0.3 \times 0.3$	$0.4 \times 0.3 \times 0.3$
Theta range for data collection (°)	2.94–32.07	3.15–32.20
Index ranges	$-16 \le h \le 15$, $-16 \le k \le 16$, $-14 \le l \le 18$	$-19 \le h \le 19$, $-18 \le k \le 17$, $-22 \le l \le 21$
Reflections collected/unique	14249/8735 ($R_{int} = 0.0390$)	23696/14650 ($R_{int} = 0.0555$)
Refinement method	Full-matrix least-squares on F^2	Full-matrix least-squares on F^2
Data/restraints/parameters	8735/0/325	14650/0/558
Goodness-of-fit on F^2	1.019	1.105
Final R indices [$I > 2\sigma(I)$]	$R_1 = 0.0442$, $wR_2 = 0.1087$	$R_1 = 0.1030$, $wR_2 = 0.2811$
R indices (all data)	$R_1 = 0.0564$, $wR_2 = 0.1178$	$R_1 = 0.1363$, $wR_2 = 0.3184$
Largest diff. peak and hole (e Å^{-3})	0.97 and −0.57	2.50 and −1.42

Table 2. Selected bond lengths (Å) and angles (°) for [NiCl(BzBudtc)(PPh_3)] and [Ni(BzBudtc)(PPh_3)$_2$]$PF_6 \cdot 0.5CH_3OH$.

[NiCl(BzBudtc)(PPh_3)]			
Ni(1)–S(1)	2.1745(10)	S(1)–Ni(1)–P(1)	94.23(2)
Ni(1)–P(1)	2.1849(11)	S(1)–Ni(1)–Cl(1)	171.20(2)
Ni(1)–Cl(1)	2.1952(10)	P(1)–Ni(1)–Cl(1)	92.49(3)
Ni(1)–S(2)	2.2224(11)	S(1)–Ni(1)–S(2)	79.02(3)
S(1)–C(1)	1.737(2)	P(1)–Ni(1)–S(2)	172.62(2)
S(2)–C(1)	1.723(2)	Cl(1)–Ni(1)–S(2)	94.53(3)
C(1)–N(1)	1.309(3)	C(1)–S(1)–Ni(1)	87.12(7)
		C(1)–S(2)–Ni(1)	85.93(7)
		S(2)–C(1)–S(1)	107.93(11)
[Ni(BzBudtc)(PPh_3)$_2$]$PF_6 \cdot 0.5CH_3OH$			
Ni(1)–S(1)	2.1890(14)	S(1)–Ni(1)–P(1)	94.52(6)
Ni(1)–P(1)	2.1989(14)	S(1)–Ni(1)–P(2)	163.65(6)
Ni(1)–P(2)	2.2188(14)	P(1)–Ni(1)–P(2)	99.77(5)
Ni(1)–S(2)	2.2468(15)	S(1)–Ni(1)–S(2)	78.60(6)
S(1)–C(1)	1.760(6)	P(1)–Ni(1)–S(2)	170.15(5)
S(2)–C(1)	1.710(5)	P(2)–Ni(1)–S(2)	88.10(6)
C(1)–N(1)	1.295(7)	C(1)–S(1)–Ni(1)	86.79(17)
		C(1)–S(2)–Ni(1)	86.2(2)
		S(2)–C(1)–S(1)	108.2(3)

at 840 cm^{-1}} was indicated [19]. IR spectra of all complexes exhibit typical dithiocarbamate ν(C–S) vibrations at 992–1011 cm^{-1} and ν(C–N) vibrations at 1500–1520 cm^{-1} [20, 21]. Square planar coordination of the nickel is supported also by electronic reflectance spectroscopy in nujol; the strong bands in the

Table 3. Possible hydrogen bonds for [NiCl(BzBudtc)(PPh_3)].

Donor-H	Donor···Acceptor	H···Acceptor	Donor-H···Acceptor
C2–H2A	C2···S1	H2A···S1 (0)	C2–H2A···S1
0.975(4)	3.108(5)	2.565(2)	115.2(2)
1.080*		2.522*	113.1*
C4–H4B	C4···N1	H4B···N1	C4–H4B···N1
0.927(3)	3.095(38)	2.723(26)	104.9(3)
1.080*		2.688*	101.8*
C6–H6B	C6···S2	H6B···S2	C6–H6B···S2
0.943(6)	3.105(4)	2.530(1)	119.5(1)
1.080*		2.466*	116.7*
C21–H21	C21···Cl1	H21···Cl1	C21–H21···Cl1
0.923(2)	3.431(2)	2.761(6)	130.3(2)
1.080*		2.663*	127.7*
C6–H6A	C6···Cl1(1)[a]	H6A···Cl1(1)[a]	C6–H6A···Cl1(1)[a]
0.968(21)	3.818(27)	2.926(6)	153.7(2)
1.080*		2.826*	152.65*

*Values normalized following G.A. Jeffrey, L. Lewis. *Carbohydr. Res.*, **60**, 179 (1978); R. Taylor, O. Kennard. *Acta Cryst.*, **B39**, 133 (1983). [a]Equivalent position (1) is at $-x+1, -y+2, -z$.

15,800–25,000 cm^{-1} region can be assigned to d–d transitions typical of square planar nickel(II) [22, 23]. Bands over 28,000 cm^{-1} are probably intraligand transitions of the S_2CN^- group [24].

^{31}P NMR spectra (table 5) of free PPh_3 and PBu_3 ligands exhibit a singlet with chemical shifts −4.5 and −30.07 ppm, respectively. These singlets were also recorded for most complexes (only **VI**, **VII** and **XI** exhibit doublets), but with larger values of chemical shift due to the electron density changes around P probably with coordination of PR_3. This effect was recently described in the literature [25, 26]. The spectra of **VII** and **X** exhibit a septet near −144 ppm, typical of PF_6^-. Comparison of δ values of **II**–**V** shows that changes of the anion (electronegativity, volume) cause significant diferences in chemical shift, increasing as $\delta\ (Cl^-) < \delta\ (NCS^-) < \delta\ (Br^-) < \delta\ (I^-)$.

The X-ray structures of **II** {[NiCl(BzBudtc)(PPh_3)], figure 1} and **VII** {[Ni(BzBudtc)(PPh_3)$_2$]$PF_6 \cdot 0.5CH_3OH$, figure 2} confirm previous conclusions about the slightly distorted square planar coordination of nickel in this type of compound. This is apparent from values of Ni–S, Ni–P and Ni–Cl bond lengths and angles in the NiS_2PCl and NiS_2P_2 chromophores (table 2). Deviations of the chromophore atoms from ideal LSQ planes are **II**: Ni(1) 0.000(4); S(1) 0.000(8); S(2) 0.000(8); P(1) −0.115(8); Cl(1) 0.231(8) Å; **VII**: Ni(1) 0.00(1); S(1) 0.00(2); S(2) 0.01(3); P(1) 0.27(2); P(2) −0.37(2) Å. A significant π-bond component in C(1)–N(1), C(1)–S(1) and C(1)–S(2) for both structures was found (table 2); bond lengths are shorter then the published values of simple σ(C–N) and σ(C–S) bonds (1.47 and 1.81 Å) [27]. For **VII**, PF_6^- is positioned out of the coordination sphere with Ni(1)–P(3) = 8.43 Å. The quality of diffraction data for **VII** was not high, but all attempts to obtain a better single crystal were unsuccessful. Significant disorder of the butyl group C(4), C(5) and CH_3OH solvate and high residual electron density values situated near sulphur atoms in the final electron density map were observed. The best convergence was reached by using 0.5 occupancy factors for disordered atoms and the methanol molecule. Therefore, only for **II** were possible hydrogen bonds calculated (table 3).

Table 4. Characterization data for the complexes.

	Colour	λ_M ($S\,cm^2\,mol^{-1}$)	IR (cm^{-1})[c]			Abs. max. $\times 10^3\,cm^{-1}$	(°C)			
			ν (C–S)	ν (C–N)			B	E_n	E_x	T_t
I	Green	0.9[a]	1008w	1512m		15.8; 20.2; 24.6; 25.6; 31.0	236.9	131.6 733.1	313.0; 331.9 445.4; 507.5	131
II	Violet	2.7[b]	998w	1500m		19.4; 28.8	174.5	206.3	240.4; 248.9 318.5; 428.4; 475.2	208
III	Violet	2.3[b]	995w	1512s		19.1; 28.1	204.0	210.6	207.7; 221.4 264.5; 437.1; 463.0	212
IV	Violet	3.2[b]	1000m	1510s		18.6; 31.1	172.6	–	180.7; 243.9; 476.1	192
V	Red	2.8[b]	996w	1508m	ν(C≡N): 2090m; ν(C–S): 840w	20.8; 30.3; 35.0	171.4	181.4	222.9; 304.8 422.1; 533.2	181
VI	Violet	127.5[a]	1008vs	1515vs	$\nu_3(ClO_4^-)$: 1089s; $\nu_4(ClO_4^-)$: 615s	19.0; 31.1				
VII	Violet	118.6[a]	1011m	1512s	$\nu(PF_6^-)$: 835vs	19.2; 31.0	169.6	–	187.4; 199.5 285.0; 444.1; 556.4	203
VIII	Red	105.3[a]	995w	1500w		18.8; 25.0; 31.2	95.4	–	116.6; 138.3; 537.3	72
IX	Light brown	112.6[a]	992m	1500m	$\nu_3(ClO_4^-)$: 1065s; $\nu_4(ClO_4^-)$: 620m	19.7; 24.6; 30.4				
X	Light brown	108.8[a]	1012w	1505m	$\nu(PF_6^-)$: 830vs	19.6; 24.5; 32.1	138.9	84.6	183.9; 275.2; 341.9	84
XI	Orange	126.4[a]	1010w	1520w		19.6; 33.1	116.5	112.5	121.5; 143.5 209.8; 551.2	114

[a]In acetone. [b]In nitromethane solution; $[Ni^{2+}] = 10^{-3}$ mol dm^{-3}. [c]Maxima in nujol. B = start of thermal decomposition, E_x = peak of exotherm, E_n = peak of endotherm, T_t = melting point.

Table 5. $^{31}P\{^{1}H\}$-NMR data for the complexes.

	Complex	δ (ppm, 300 K)		δ (ppm, 320 K)
I	$[Ni(BzBudtc)_2]$			
II	$[NiCl(BzBudtc)(PPh_3)]$	20.88(s)		
III	$[NiBr(BzBudtc)(PPh_3)]$	24.48(s)		
IV	$[NiI(BzBudtc)(PPh_3)]$	31.08(s)		
V	$[Ni(NCS)(BzBudtc)(PPh_3)]$	22.53(s)		
VI	$[Ni(BzBudtc)(PPh_3)_2]ClO_4$	31.46(d)		31.20(s)
VII	$[Ni(BzBudtc)(PPh_3)_2]PF_6$	31.44(d)	−143.98 (septet)	31.21(s)
VIII	$[Ni(BzBudtc)(PPh_3)_2]BPh_4$	29.25(s)		29.25(s)
IX	$[Ni(BzBudtc)(PBu_3)_2]ClO_4$	23.76(s)		23.74(s)
X	$[Ni(BzBudtc)(PBu_3)_2]PF_6$	11.81(s)	−144.07(septet)	11.80(s)
XI	$[Ni(BzBudtc)(PBu_3)_2]BPh_4$	11.63(d)		11.67(s)

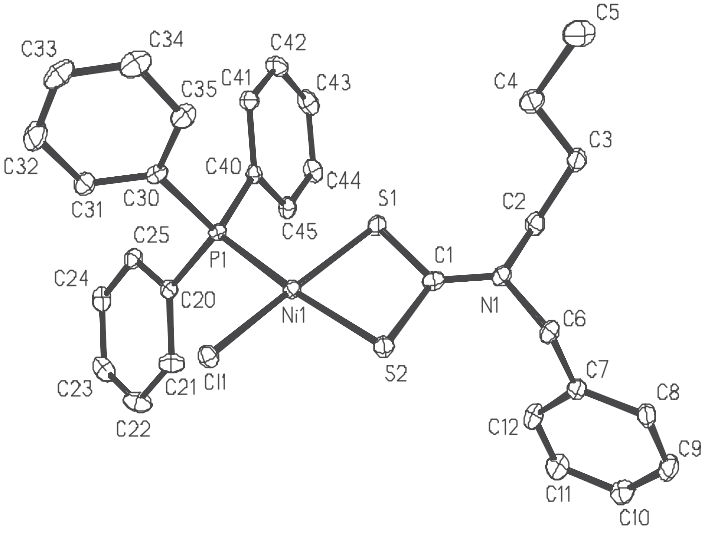

Figure 1. ORTEP drawing of $[NiCl(BzBudtc)(PPh_3)]$ with the atom labelling scheme. Thermal ellipsoids are drawn at the 40% probability level and hydrogen atoms are omitted for clarity.

Thermal analyses (table 4) show that the most stable complex is **I**. Its melting point is connected with a small sharp endotherm at 132°C. Decomposition starts at 237°C and is accompanied by three small exotherms. The exotherm at 508°C is caused by the formation of NiS_2 (thermally stable in the range 640–668.3°C). The following reaction gives NiS (mass loss Calcd/found: 83.0/82.9%, endotherm at 733°C), which is thermally stable to 1050°C (max. temperature of instrument). These results are comparable with data for similar complexes [28]. Compounds **II**–**V**, **VII**, **VIII**, **X** and **XI** decompose in the range 95–204°C without thermally stable intermediates. Endotherms at 85 to 211°C are connected with melting with decomposition. The most interesting is the last compound, **XI**. In this case, a small mass increase in TG at 120°C and an exotherm at 122°C were recorded. This is known for Ni(II) dithiocarbamates with phosphines [4, 30] and is explained by insertion of oxygen into the Ni–P bond [29]. This reaction can be probably assumed (see sharp exotherms, table 4) for remaining complexes but mass increase was not observed due to simultaneous decomposition. Compounds **VI** and **IX** containing perchlorate were not studied for safety reasons.

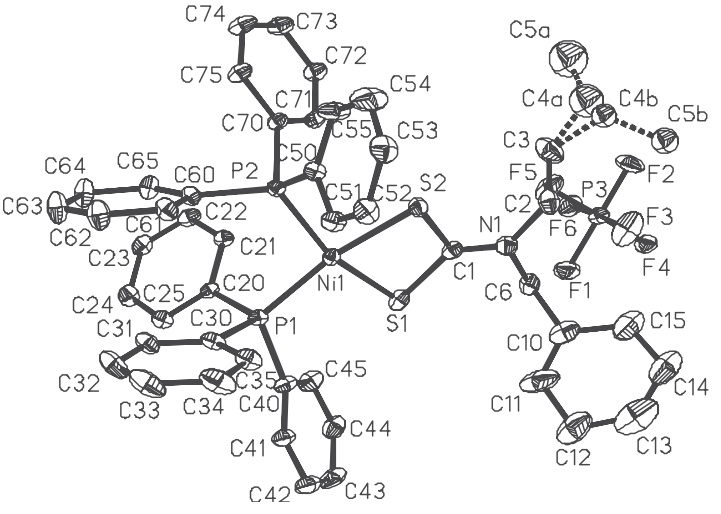

Figure 2. ORTEP drawing of $[Ni(BzBudtc)(PPh_3)_2]PF_6 \cdot 0.5CH_3OH$ with the atom labelling scheme. Thermal ellipsoids are drawn at the 40% probability level and hydrogen atoms and included solvent molecules are omitted for clarity.

Table 6. Characteristic temperatures (°C) and kinetic parameters for graphite oxidation using selected complexes.

Complex	T_p	T_m	T_k	$T_k - T_p$
0	751	803	838	87
I	703	796	841	138
IV	677	819	861	184
VI	686	822	863	177
X	684	803	849	165

Complex	Step	n	A (s^{-1})	E (kJ mol^{-1})	w (%)
0		0.9	$1.40 \cdot 10^{10}$	254	
I	I	1.0	$4.36 \cdot 10^{6}$	171	25.8
	II	1.0	$1.63 \cdot 10^{9}$	238	74.1
IV	I	0.9	$2.23 \cdot 10^{6}$	166	38.4
	II	0.9	$1.24 \cdot 10^{8}$	216	61.6
VI	I	1.5	$6.00 \cdot 10^{6}$	198	60.8
	II	0.6	$3.31 \cdot 10^{8}$	219	39.1
X	I	1.3	$2.05 \cdot 10^{6}$	180	55.4
	II	1.0	$1.67 \cdot 10^{10}$	262	44.6

T_p = start of oxidation, T_m = oxidation speed maximum, T_k = end of oxidation, n = reaction order, A = frequency factor, E = activation energy, w = mass of sample oxidized.

The influence on graphite oxidation was studied. From DTG curves and characteristic temperatures on TG curves (table 6) it is apparent that the presence of small amounts of Ni(II) complexes exerts a significant influence on graphite oxidation. All complexes cause a significant decrease (50 to 70°C) in oxidation start (but not end) temperature in comparison to pure graphite (**0**). Graphite oxidation proceeds with complexes in two continuous steps. In the first, the maximum reaction speed is at lower temperature. In the second, the maximum rate corresponds to that of pure graphite

(see T_m values), but T_k values for samples with complexes are a little higher than for pure graphite and the oxidation process is characterized by a larger temperature interval ($T_k - T_p$). The ratio of the first/second step for **I** is lower than for **IV**, **VI** and **X**. Kinetic parameters (table 6) were calculated for one-step oxidation (sample **0**, pure graphite) and two-step oxidation (samples with complexes **I, IV, VI**, **V** and **X**). For all complexes, the results show that the mechanism of oxidation for the first and second step is different. The first is characterized by E values less than $200\,kJ\,mol^{-1}$ and A about $10^6\,s^{-1}$, which are quite different to the pure graphite parameters (these values correspond rather to the parameters of the second step). The catalytic influence can be probably explained by formation of common species with all complexes. Different catalytic effects are connected with kinetic factors. The increase of reaction order of the first step in the presence of complexes **VI** and **X** shows that the presence (even of a trace amount) of complex exhibits a remarkable catalytic influence on the mechanism of graphite oxidation. This is in accord with previous results for unsymmetrical Ni(II) dithiocarbamates [8].

Supplementary data

Crystallographic data are deposited at the Cambridge Crystallographic Data Centre, No. CCDC 298862 (**II**) and 299795 (**VII**). Copies of the data can be obtained free of charge on application to CCDC, 12 Union Road, Cambridge CB2 1EZ, UK (Fax: +441223/336033; E-mail: deposit@ccdc.cam.ac.uk or http://www.ccdc.cam.ac.uk).

Acknowledgements

The authors would like to thank the Ministry of Education, Youth and Sports (grant No. MSM 6198959218) for financial support of this work. We also thank Prof. Zdeněk Trávníček for X-ray measurements and data reduction, Dr. Igor Popa for NMR spectra and Assoc. Prof. Zdeněk Šindelář for magnetochemical measurements.

References

[1] A. Manohar, V. Venkatachalam, R. Ramalingam, U. Casellato, R. Graziani. *Polyhedron*, **16**, 1971 (1997).
[2] S. Thirumaran, K. Ramalingam. *Trans. Met. Chem.*, **25**, 60 (2000).
[3] R. Pastorek, J. Kameníček, Z. Trávníček, J. Husárek, N. Duffy. *Polyhedron*, **18**, 2879 (1999).
[4] R. Pastorek, J. Kameníček, J. Husárek, M. Pavlíček, Z. Šindelář, Z. Žák. *Polish J. Chem.*, **76**, 1545 (2002).
[5] B. Cvek, J. Husárek, R. Pastorek, Z. Šindelář. *Acta Univ. Palacki. Olom. Chem.*, **43**, 68 (2004).
[6] J. Husárek, R. Pastorek, M. Maloň, Z. Šindelář, M. Pavlíček. *J. Serb. Chem. Soc.*, **69**, 1053 (2004).
[7] R. Pastorek, J. Kameníček, B. Cvek, V. Slovák, M. Pavlíček. *J. Coord. Chem.*, **59**, 911 (2006).
[8] R. Pastorek, J. Kameníček, H. Vrbová, V. Slovák, M. Pavlíček. *J. Coord. Chem.*, **59**, 437 (2006).
[9] In *Gmelins Handbuch der Anorganischen Chemie, Nickel*, C. Teil (Ed.), Lief. 2, p. 1043, Verlag Chemie, Weinheim (1969).
[10] R. Přibil. *Komplexometrické Titrace*, p. 22, SNTL, Praha (1955).
[11] M. Jureček. *Organická Analýza II*, p. 140, ČSAV, Praha (1957).
[12] V. Slovák. *Thermochim. Acta*, **372**, 175 (2001).
[13] G.M. Sheldrick. *SHELXS-97, Acta Crystallogr.*, **A46**, 467 (1990).

[14] G.M. Sheldrick. *SHELXL-97, Program for Crystal Structure Refinement*, University of Göttingen, Germany (1997).
[15] N. Walker, D. Stuart. *Acta Crystallogr.*, **A39**, 158 (1983).
[16] M. Nardelli. *PARST 95, J. Appl. Cryst.*, **28**, 659 (1995).
[17] R.P. Scholer, E.A. Merbach. *Inorg. Chim. Acta*, **15**, 15 (1975).
[18] L. Ballester, A. Gutierrez, M.F. Perpinan, C. Ruiz-Valero. *Polyhedron*, **15**, 1103 (1996).
[19] I.E. Černikova, I.A. Chartonik, D.S. Umrejko, A.B. Kavrikov, V.I. Afanov. *Koord. Chim.*, **15**, 1695 (1989).
[20] C.A. Tsipis, D.P. Kessissoglou, G.A. Katsoulos. *Chim. Chron., New Series*, **14**, 195 (1985).
[21] S.V. Larionov, L.A. Patrina, I.M. Oglezneva, E.M. Uskov. *Koord. Chim.*, **10**, 92 (1984).
[22] A.B.P. Lever. *Inorganic Electronic Spectroscopy*, p. 534, Elsevier, Amsterdam (1984).
[23] C.A. Tsipis, D.P. Kessissoglou, G.E. Manoussakis. *Inorg. Chim. Acta*, **65**, L137 (1982).
[24] C.A. Tsipis, I.E. Meleziadis, D.P. Kessissoglou, G.A. Katsoulos. *Inorg. Chim. Acta*, **90**, L19 (1984).
[25] B.A. Prakasam, K. Ramalingam, G. Bocelli, R. Olla. *Z. Anorg. Allg. Chem.*, **630**, 301 (2004).
[26] B.A. Prakasam, K. Ramalingam, M. Saravanan, G. Bocelli, A. Cantoni. *Polyhedron*, **23**, 77 (2004).
[27] D.R. Lide (Ed.). *Handbook of Chemistry and Physics*, 73rd Edn, CRC Press, Boca Raton, FL (1992).
[28] R. Pastorek, F. Březina, J. Pokludová. *Acta Univ. Palacki. Olom.*, **91**, 17 (1988).
[29] F. Březina, E. Benátská. *J. Thermal Anal.*, **22**, 75 (1981).
[30] R. Pastorek, J. Kameníček, B. Cvek, M. Pavlíček, Z. Šindelář, Z. Žák. *J. Coord. Chem.*, **56**, 1123 (2003).